AIAA 96-1962

Far-Field Turbulent Vortex-Wake/Exhaust Plume Interaction for Subsonic and HSCT Airplanes

Osama A. Kandil, Ihab Adam and Tin-Chee Wong
Aerospace Engineering Department
Old Dominion University, Norfolk, VA 23529

27th AIAA Fluid Dynamics Conference
June 17-20, 1996 / New Orleans, LA

FAR-FIELD TURBULENT VORTEX-WAKE/EXHAUST PLUME INTERACTION FOR SUBSONIC AND HSCT AIRPLANES

Osama A. Kandil*, Ihab Adam** and Tin-Chee Wong***
Old Dominion University, Norfolk, Virginia 23529

ABSTRACT

Computational study of the far-field turbulent vortex-wake/exhaust plume interaction for subsonic and high speed civil transport (HSCT) airplanes is carried out. The Reynolds-averaged Navier-Stokes (NS) equations are solved using the implicit, upwind, Roe-flux-differencing, finite-volume scheme. The two-equation shear stress transport model of Menter is implemented with the NS solver for turbulent-flow calculation. For the far-field study, the computations of vortex-wake interaction with the exhaust plume of a single engine of a Boeing 727 wing in a holding condition and two engines of an HSCT in a cruise condition are carried out using overlapping zonal method for several miles downstream. These results are obtained using the computer code FTNS3D. The results of the subsonic flow of this code are compared with those of a parabolized NS solver known as the UNIWAKE code.

INTRODUCTION

The volume of civil air transport of subsonic aircraft has increased at an alarming rate. With this increase in air traffic, several hazardous effects have recently become of primary concern. First, the landing and take-off operations safety at busy airports of small and medium size aircrafts become hazardous when they encounter high-intensity turbulent vortices emanating from large aircraft. The trailing aircraft, under the influence of those vortex trails, could suffer high rolling moments, loss of climb and structural damages. The vortices persist up to a few miles and several minutes before they decay.

Second, the adverse effects of the engine exhaust of both subsonic and supersonic aircraft on the stratosphere and troposphere during cruise and holding conditions are of primary atmospheric concern. A complex flow regime develop behind those aircraft which include the exhaust jet plume and the wake vortices that entrain the exhaust plumes and eventually break-up producing exhaust-atmosphere mixing region. Substantial adverse effects on the stratosphere and troposphere are expected when the new fleet of High Speed Civil Transport (HSCT) is introduced in the early years of the next century. Recent research efforts are currently directed at understanding the adverse atmospheric effects of exhaust products from subsonic and supersonic civil transport aircrafts. These efforts include predicting the effects of exhaust plume on the dynamical, chemical and radiative stratospheric processes. A recent NASA report on these issues is published under the Atmospheric Effects of Aviation Project (AEAP), Ref. 1.

The origins of these hazardous effects are the vortex-wake flows and the engine jet exhaust plume and its interaction with the vortex-wake flows. The vortex-wake flows include the tip-vortex development and roll-up formation while the jet exhaust plume include exhaust products, temperature field, and their fluid mechanics. At some distance downstream, the vortex-wake flows entrain the exhaust plume and later-on the vortex-wake breaks up and dilutes the exhaust plume in the stratosphere.

The literature shows some experimental and computational investigations that model and analyze the roll-up of a tip vortex, the wake-vortex interaction, and the merging and decay, as well as the hazardous effects of these phenomena on trailing aircraft.

Mathematical models and computational methods were developed with inviscid analysis[2-5]. Although an inviscid model cannot describe the aging of the wake including its diffusion, it is still capable of representing the wake shape and its dynamics. The mathematical models used in the above references were based on the use of the point-vortex method to compute the motion of a finite number of point vortices. The three-dimensional inviscid model which is based on the nonlinear vortex-lattice method, was used to compute the interference flow between the wings and the vortex-wake flows and to examine their hazardous effects[6].

Viscous interactions of vortex wakes and the effects of background turbulence, wind shear, and the ground on two-dimensional vortex pairs were presented in Refs. 7 and 8. The computer program used for these calculations is known as the UNIWAKE code. The interaction, merging, and decay of vortices in two- and three-dimensional spaces were studied in Refs. 9 and 10. A comprehensive review on the subject of viscous vortical flows can be found in a book by Ting and Klein[11]. To estimate the effects of density stratification, turbulence, and Reynolds number on vortex wakes, an approximate model was recently developed by Greene[12]. Later on, Greene and his coworkers[13] presented selected results for different aircraft vortices, including a juncture vortex, a lifting-wing vortex, and a wake vortex.

In recent papers by the present authors[14, 15], the compressible Reynolds-averaged NS equations were used to compute and analyze vortex-wake flows of isolated and interacting wings. The emphasis of the paper was to study the effects of the near-wake vortex flow on a small follower wing for two cases of flow interference. The flux limiter in the flow solver was turned on and off to study its numerical diffusive effect. The solution obtained with the full NS equations without a flux limiter gave the least numerically diffused tip-vortex core

* Professor, Eminent Scholar and Chair of Aerospace Engineering Department, Associate Fellow AIAA.
** Graduate Student, Aerospace Engineering Department, Member AIAA.
***Research Assistant Professor, Aerospace Engineering Department, Member AIAA.

in comparison with those solutions for which a flux limiter was used. The multidisciplinary interaction of the aerodynamics and rigid-body dynamics between a single tip vortex and a trailing wing was also computationally investigated by the present authors[16].

Very recently, research interest has also been focused on the near-field and far-field vortex-wake interaction with the engine exhaust plume including vortex-wake break up for both subsonic and high speed civil transport (HSCT) aircraft. Computational fluid dynamics plays a significant role in the prediction of the near-field and far-field vortex-wake flows. Once this is accomplished, the next step is to include the exhaust plume products and chemical reactions, and its interaction with the vortex-wake flows including vortex-wake break-up.

Recently, more advanced turbulence models became readily available for use with NS solvers. In Ref. 17 by authors, the algebraic Baldwin and Lomax (BL) turbulence model[18], the one-equation Spalart and Allmaras (SA) model[19], and the two-equation $k\omega$ (KW) model developed by Menter[20] were used to study the tip-vortex and wake flows and their interaction with the temperature field of an exhaust plume of a Boeing 727. Three key ingredients were considered for achieving accurate prediction of these flows. These are the grid fineness, turbulence model and computational efficiency. The results using different models were validated with the available experimental data.

In this paper, computational investigations of the far-field turbulent vortex-wake/exhaust jet plume interaction for a Boeing 727 tip vortex and a single engine, and a HSCT vortex-wake and twin engines are carried out. The Boeing 727 is in a holding condition and the HSCT is in a cruise condition. An overlapping zonal method is used to carry out the computations for several miles downstream. The present computational results of the subsonic flow case are compared with those of the UNIWAKE code. Development of lateral flow asymmetry is also investigated.

FORMULATION

Two sets of the NS equations are used for these investigations: a compressible set and an incompressible set. The compressible set is solved using a computer program known as the FTNS3D code, which is used in reference[16]. This is a modified version of the well known CFL3D code. The incompressible set is solved using a computer program known as the UNIWAKE code, which is used in References 7 and 21.

The FTNS3D solver, described in detail in reference 16, uses an upwind, flux-difference splitting, finite-volume scheme to solve for the unsteady, compressible, Reynolds-averaged NS equations. For the exhaust plume/tip vortex or vortex-wake interaction cases, the buoyancy body force caused by temperature difference, between the exhaust plume and the ambient conditions, is added as a source term without any approximation in the NS equations. For all results in this paper, upwind-biased spatial differencing is used for the inviscid terms, and flux limiter is not used. The viscous terms are differenced using second-order accurate central differencing. The resulting difference equations are solved implicitly in time with the use of the three-factor approximate factorization scheme. The two-equation turbulence model (KW) of Menter is used with the NS equations. Partial differential equations for the turbulence model are solved sequentially at each time step thereafter.

The UNIWAKE solver consists of four computational modules: (1) Vortex Lattice: A program to compute the lift circulation distribution on an aircraft wing, which is based on the given aerodynamic parameters and wing planform shape. (2) Betz: A program to generate the initial position and strength of rolled-up trailing edge vortices, given the lift circulation distribution. (3) Wake: A program to merge and decay these vortices downstream, interacting with engine jet exhaust temperature and chemical products, by solving the incompressible parabolized NS equations with fourth-order compact scheme in uniformly Cartesian system. The second derivatives in the streamwise direction is neglected in the governing equations. The effects of the turbulence are included through the algebraic Reynolds stress turbulence model. (4) Pinch: A program to follow the inviscid line vortex filament interaction of these vortices to instability and pinching, utilizing curved vortex elements. Recently, some aspects of the compressibility and density variations are taken into account in the latest version of UNIWAKE. It should be noted that the buoyancy body force caused by temperature difference is based on the Boussinesq approximations which are not valid for high temperature differences. The detail of the governing equations and recent enhancements can be found in Ref. 21.

BOUNDARY AND INITIAL CONDITIONS

Boundary conditions are explicitly implemented. They include inflow-outflow conditions. At the inflow boundaries, the velocity profiles and pressure are prescribed and the Riemann-invariant boundary-type conditions are used. Temperature distribution is specified for the engine exhaust plume(s). At the outflow boundaries, conditions are extrapolated from the interior domain. At the geometric plane of symmetry, periodic conditions is set for symmetric flow problems. The initial conditions correspond to the uniform-flow conditions

RESULTS AND DISCUSSION

Far-Field Flow of Tip-Vortex/Exhaust Plume For a Boeing 727 (One-Side Flowfield)

The tip-vortex/exhaust jet plume interaction of a Boeing 727 wing and a single engine is considered. The study addresses the computation and analysis of the tip-vortex interaction with the exhaust jet plume temperature field for a long distance downstream of the wing. The tip-vortex of the Boeing 727 wing is assumed to be fully rolled-up and the generation region is not included in the computation. The inflow velocity and pressure profiles are generated using the vortex-lattice and Betz modules of the UNIWAKE.

The tip-vortex flow is assumed fully turbulent with a Reynolds number of 1 x 10^6, based on the semi-span of the wing, and the flow Mach number is 0.3. The tip-vortex and exhaust plume are located at y/s = 0.76, z/s = 0.0, and y/s = 0.4, z/s = -0.1, respectively. The peak temperature at the center of the engine is two times the ambient temperature. The crossflow velocity (Vc), and temperature (T) contour distributions at x/s = 0.0 are shown in Fig. 1.

The NS equations are used to compute the development of this vortex and its interaction with the plume for a long distance, up to x/s = 130. The computations of the FTNS3D solver are carried out using an overlapping zonal method and the schematic sketch is shown in Fig. 2. For each stage of computation, a fine grid zone is used. The downstream distance (a) and the overlapping or buffer zone (b) should be chosen such that the downstream effects are minimized. For this case, the following values are chosen; a/s=8.0, b/s=2.0, and Xmax/s=130 (equivalent to 1.18 mile behind the inflow plane). The computations are carried out for the right side of the flowfield assuming flow symmetry. A rectangular grid of 201 x 41 x 51 grid points in x, y, and z directions, respectively, are used for each zone.

The computations are carried out starting from the inflow station of x/s = 0.0 up to x/s = 130 using the FTNS3D with the KW turbulence model and the UNIWAKE solvers on the same grid resolution in the crossflow plane. The results of the T and Vc contours at selected chord stations with FTNS3D (left column) and UNIWAKE (right column) solvers are shown in Figs. 3-5. All the results are plotted in reference to the origin and the corresponding axes at the inflow section. The results show the evolution of the tip-vortex interaction with the temperature field of the plume as it is advanced downstream.

The results of the FTNS3D code show that tip-vortex center first moves upward and inward (due to the buoyancy effect of the temperature field of the plume), and then descends and moves toward the plane of symmetry as it advances in the downstream direction. During the tip vortex motion, the exhaust plume is wrapped around it and its flow is entrained in the tip-vortex. On the other hand, the UNIWAKE results show that the tip-vortex center continuously descends and stays almost at the same lateral location of y/s = 0.76. Since the UNIWAKE code is a space-marching NS solver, the step size in the streamwise direction is determined based on extrapolated changes in the flow variables at each station. The code also has a dynamic adjustment that seeks to retain the perceived vortical mean location at the position of z/s = 0.0. The discrepancies between the two solvers are due to the use of the approximate parabolized NS equations of the UNIWAKE code and the fully three-dimensional NS equations of the FTNS3D code. The results with the UNIWAKE solver show more diffusion as compared with the FTNS3D results. One of the numerical parameters known as the turbulent macroscale (Λ) in the UNIWAKE code has to be adjusted from the default values of 0.2 to 0.04 in order to obtain adequate less-diffused results. The larger values of Λ (results are not shown here) show even more diffusive effect as compared with the FTNS3D results.

Far-Field Flow of Tip-Vortex/Exhaust Plume for a Boeing 727 (Two-Side Flowfield):

In this case the two sides (right and left) of the flowfield are computed, instead of the one-side computations of the previous case, in an attempt to capture possible evolution of flow asymmetry downstream. For this case, a/s=20 and b/s=12 for each computational zone. A rectangular grid of 201x81x51 in x, y, and z directions, respectively is used. The grid is coarsened in the axial direction in the overlapping zone (b/s=12). The inflow conditions as well as the flow conditions are the same as those of the previous case. The computations are carried out up to X_{max}/s=110. The results of this case are shown in Fig. 6. It is observed that no flow asymmetry has evolved up to the last-computed downstream station. Comparison of these results with those of the previous case shows small differences in the V_c and T contours. The reason behind these small differences is the longer zone size and overlapping zone used in this case in comparison with the previous case. The lateral separation distance between the tip vortices was reduced down from y/s=1.54 to y/s=0.8 and no flow asymmetry was captured (results are not shown).

Far-Field Flow of Vortex-Wake/Two Engine Plumes for HSCT (One-Side Flowfield):

In this case the far-field interaction of a vortex-wake flow of a generic HSCT with the exhaust plume temperature fields of two engines is considered. Figure 7 shows the inflow plane with the vortex-wake flow in the z/s=0.0 plane extending from y/s=0.0 to y/s=1.0. The centers of the two engine exhaust plumes are located at y/s=0.3 and y/s=0.6 in the z/s=0.0 plane. The vortex-wake flow is assumed fully turbulent with a Reynolds number of $8x10^7$, based on the wing semispan, and the flow Mach number is 2.4. Figure 7 shows the crossflow velocity (V_c) and temperature (T) contours.

The NS equations are used to compute the development of this flow and its interaction with the temperature fields of the plumes for a long distance in the downstream direction, up to x/s=150. Since the flow is supersonic, no overlapping zone is used. In this case, the following values are chosen; a/s=10.0, b/s=0.0, and X_{max}/s=150. A rectangular grid of 161x77x97 grid points in x, y, and z directions, respectively, are used.

Figures 7–10 show the crossflow results of V_c and T at selected chord stations. The results show the evolution of the vortex-wake flow and its interaction with the exhaust plume temperature fields. At x/s=2.0, the exhaust plumes deform laterally while the outboard region of the vortex-wake deforms in the upward direction. At the downstream chord stations, x/s=6.0 to x/s=34.0, the exhaust plumes merge together and stretch while rotating under the influence of a stretching and rotating vortex-wake flow. At x/s=44.0, the outboard side of the vortex-wake rolls-down in the counter-clockwise direction and at x/s=64.0, the inboard side of the vortex-wake rolls-up in the counter clockwise direction too. The exhaust plume temperature-field takes this shape of two counter-clockwise roll-down and roll-up vortices which are connected with a vortex sheet. This system extends from z/s=–0.5 to z/s=0.5

and the roll-down and roll-up vortex centers are located at y/s=0.5, z/s=0.3, for the upper vortex, and y/s=0.65, z/s=-0.4 for the lower vortex. These vortices separate at z/s=84.0, rotate around each other at x/s=114 and merge at x/s=144. The vortices descend and move toward the plane of symmetry, and the exhaust plume flow is fully entrained in the vortex flow.

Far-Field Flow of Vortex-Wake/Two Engine Plumes for HSCT (Two-Sides Flowfield with Reduced Lateral Distance)

In an attempt to capture any possible flow asymmetry, the development of the flowfield in the downstream direction is carried out using the two-sides flowfield computations and reduced extension of the vortex-wake and the exhaust plumes. On each side, the vortex-wake extends from y/s=0.0 to y/s=0.5 in the inflow station. Flow conditions are the same as those of the previous case. The calculations are carried in the downstream direction up to x/s=60.0. The results of the V_c and T contours are shown in Fig. 10. It is noticed that no flow asymmetry has been captured up to the computed chord station. It is also noticed that the vortex roll-up develops only for the outboard side of the vortex-wake. At x/s=24.0, it is noticed that flow detrainment develops.

CONCLUDING REMARKS

The computational solution of the compressible, Reynolds-averaged Navier-Stokes equations is used to predict the far-field vortex wake/exhaust plume turbulent flow interaction. The two-equation turbulent modal of Menter is used for turbulent flow calculations. Computational results have been presented for two main applications. The first application is the interaction of tip-vortex flow of a Boeing 727 wing with the temperature field of exhaust jet plume of a single engine. The second application is the interaction of the vortex-wake flow of a HSCT wing with the temperature field of two engine exhaust jet plumes. The computations have been carried out for more than one mile in the downstream direction using an overlapping zonal method.

For the Boeing 727 tip vortex/exhaust plume interaction, it has been shown that the tip vortex moved first in the upward direction then it descended and moved toward the plane of geometric symmetry. The exhaust plume flow wrapped around the tip-vortex, and later on it was entrained in the tip-vortex flow. Comparison of the present results with those of the UNIWAKE shows that the UNIWAKE results suffer from numerical dissipation as well as the approximate equations used. The two-side flowfield computations have not developed flow asymmetry, even when the lateral separation distance was reduced. For the HSCT vortex-wake/exhaust plumes interaction, it has been shown that the vortex-wake deforms and forms two counter-clockwise rotating vortices which separate, and later on they merge. The exhaust plumes follow the motion of the vortex-wake and their flows are entrained with the two vortices. For the two-side flowfield calculations with reduced lateral distance, no flow asymmetry was captured. Flow detrainment has been captured. Research work is underway to add chemical reactions and species flow to the exhaust plume(s).

ACKNOWLEDGEMENT

This work is supported by the NASA Langley Research Center under Grant No. NAG-1-994. The computational resources provided by the NAS Center at Ames and the NASA Langley Research Center are appreciated and recognized.

REFERENCES

1. Stolarski, R. S. and Wesoky, H. L., Editors, "The Atmospheric Effects of Stratospheric Aircraft: A Fourth Program Report," NASA Ref. Pub. 1359, January 1995.

2. Chorin, A. J. and Bernard, P. S., "Discretization of a Vortex Sheet, with an Examples of Roll-Up," *Journal of Computational Physics*, Vol. 13, Nov. 1973, pp. 423-429.

3. Hackett, J. E. and Evans, M. R., "Vortex Wakes Behind High Lift Wings," *Journal of Aircraft*, Vol. 11, July 1974, pp. 397-400.

4. Iversen, J. D. and Bernstein, S., "Trailing Vortex Effects on Following Aircraft," *Journal of Aircraft*, Vol. 11, Jan. 1974, pp. 60–61.

5. Rossow, V. J., "Inviscid Modelling of Aircraft Trailing Vortices," Proceedings of NASA Symposium on Wake Vortex Minimization," Washington, D. C., Feb. 1976, pp. 4–54.

6. Kandil, O. A., Mook, D. T., and Nayfeh, A. H., "Application of the Nonlinear vortex-Lattice Concept to Aircraft-Interference Problems," Advances in Engineering Science, NASA CP-2001, Vol. 4, Nov. 1976, pp. 1321–1326.

7. Bilanin, A. J., Teske, M. E., and Williammson, G. G., "Vortex Interactions and Decay in Aircraft Wakes," *AIAA Journal*, Vol. 15, No. 2, Feb. 1977, pp. 250–260.

8. Bilanin, A. J., Teske, M. E., and Hirsh, J. E., "Neutral Atmospheric Effects on the Dissipation of Aircraft Vortex Wakes," *AIAA Journal*, Vol. 16, No. 9, Sept. 1978, pp. 956–961.

9. Liu, C. H., Krause, E., and Ting, L., "Vortex Dominated Flow with Viscous core Structure," AIAA 85–1556, July 1985.

10. Liu, C. H., Tavantzis, J., and Ting, L., "Numerical Studies of Motion and Decay of Vortex Filaments-Implementing the Asymptotic Analysis," *AIAA Journal*, Vol. 24, 1986, pp. 1290–1297.

11. Ting, L. and Klein R., *Viscous Vortical Flows*, Lecture Notes in Physics, Vol. 374, Springer-Verlag Berlin Heidelberg, 1991.

12. Greene, G. C., "An Approximate Model of Vortex Decay in the Atmosphere," *Journal of Aircraft*, Vol. 23, No. 7, July 1986, pp. 566–573.

13. Greene, G. C., Lamar, J. E., and Kubendran, L. R., "Aircraft Vortices: Juncture, Wing and Wake," AIAA Paper 88–3743, July 1988.

14. Kandil, O. A., Wong, T. C., and Liu, C. H., "Analysis and Computation of Trailing Vortices and Their Hazardous Effects," FAA International Symposium, Washington, D.C., Oct. 29–31, 1991, vol. 2, pp. 36.1–36.24.

15. Wong, T. C., Kandil, O. A., and Liu, C. H., "Computation of Wake-Vortex Flows and Control of Their Effects on Trailing Wings," AIAA 4429–92–CP, Aug. 1992, Vol. 1, pp. 280–292.

16. Kandil, O. A., Wong, T. C., and Liu, C. H., "Turbulent Flow over a 747/747 Generator/Follower Configuration and its Dynamic Response," AIAA 94–2383, June 1994.

17. Kandil, O. A., Wong, T. C., Adam I., and Liu, C. H., "Prediction of Near and Far-Field Vortex Wake Turbulent Flows," AIAA 95-3470-Cp, AIAA Atmospheric Flight Mechanics Conference, Baltimore, MD, August 7–9, 1995, pp. 412–425.

18. Baldwin, B., and Lomax, H., "Thin Layer Approximation and Algebraic Model for Separated Turbulent Flow," AIAA 78–257, Jan. 1978.

19. Spalart P. R., and Allmaras, S. R., "A One-Equation Turbulence Model for Aerodynamics Flows," AIAA 92–0439, Jan. 1992.

20. Menter, F. R., and Rumsey, C. L., "Assessment of Two-Equation Turbulence Models for Transonic Flow," AIAA 94–2343, June 1994.

21. Quackenbush, T. R., Teske, M. E., and Bilanin, A. J., "Enhancement of UNIWAKE Exhaust Dynamics and Chemistry," C.D.I. Report No. 94–04.

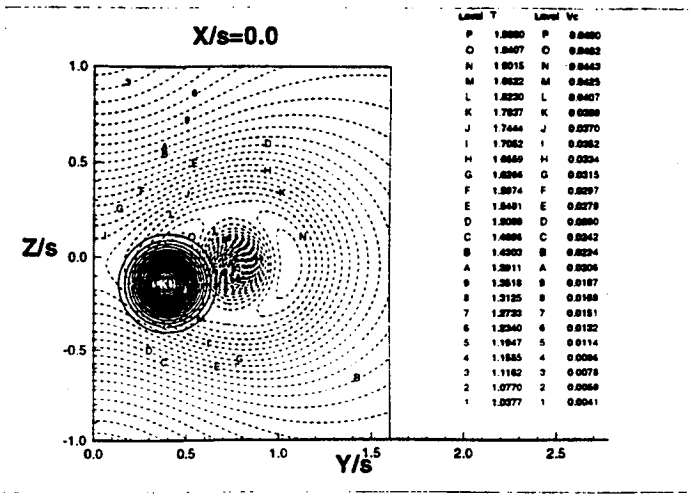

Figure 1: Crossflow velocity and temperature contours at the inflow section.

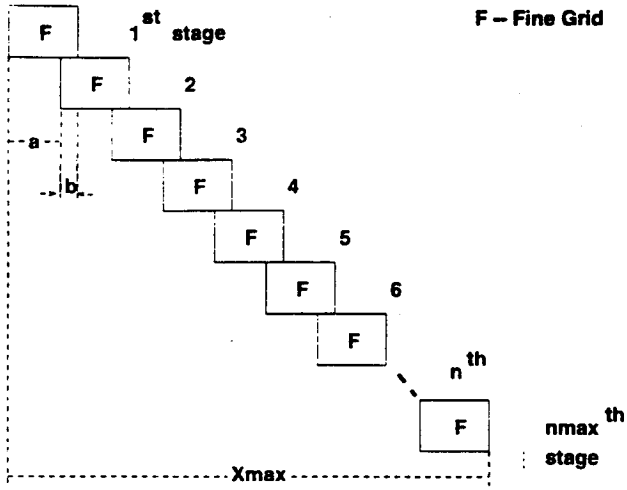

Figure 2: Schematic sketch of the overlapping zonal method.

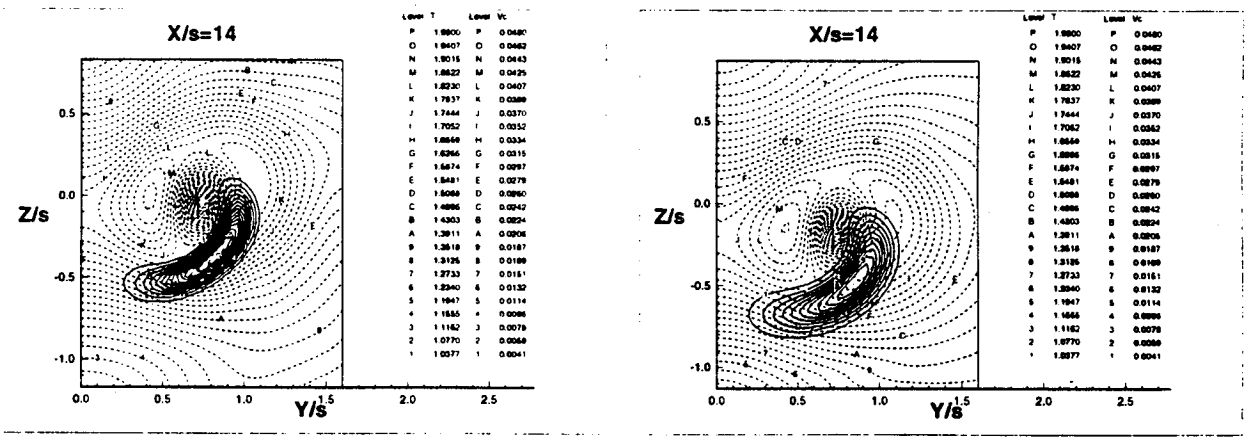

Figure 3: Comparison of crossflow T and Vc contours at one downstream station; left-FTNS3D, and right-UNIWAKE. (One-side flowfield).

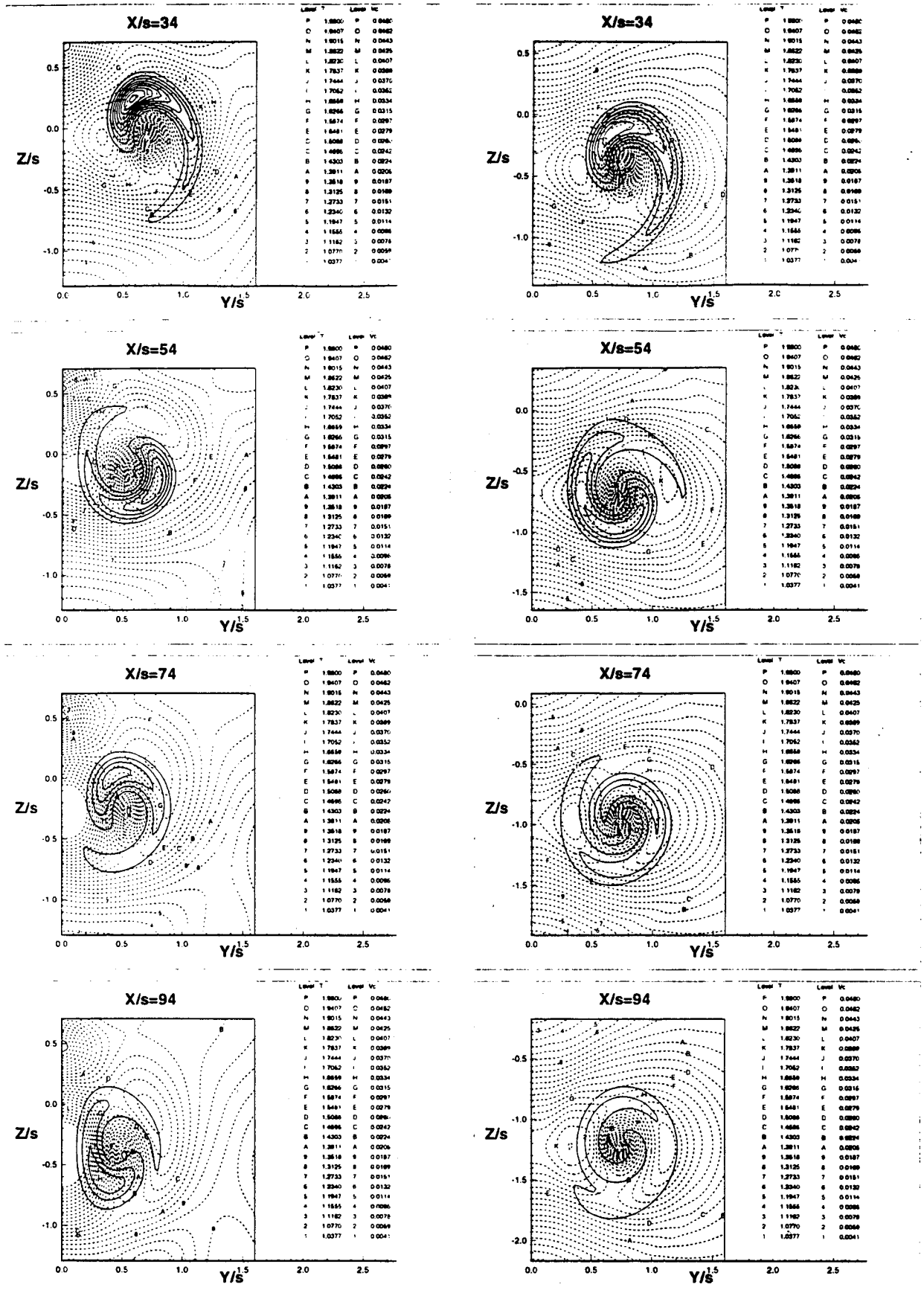

Figure 4: Comparison of crossflow T and Vc contours at four downstream stations; left-FTNS3D, and right-UNIWAKE. (One-side flowfield).

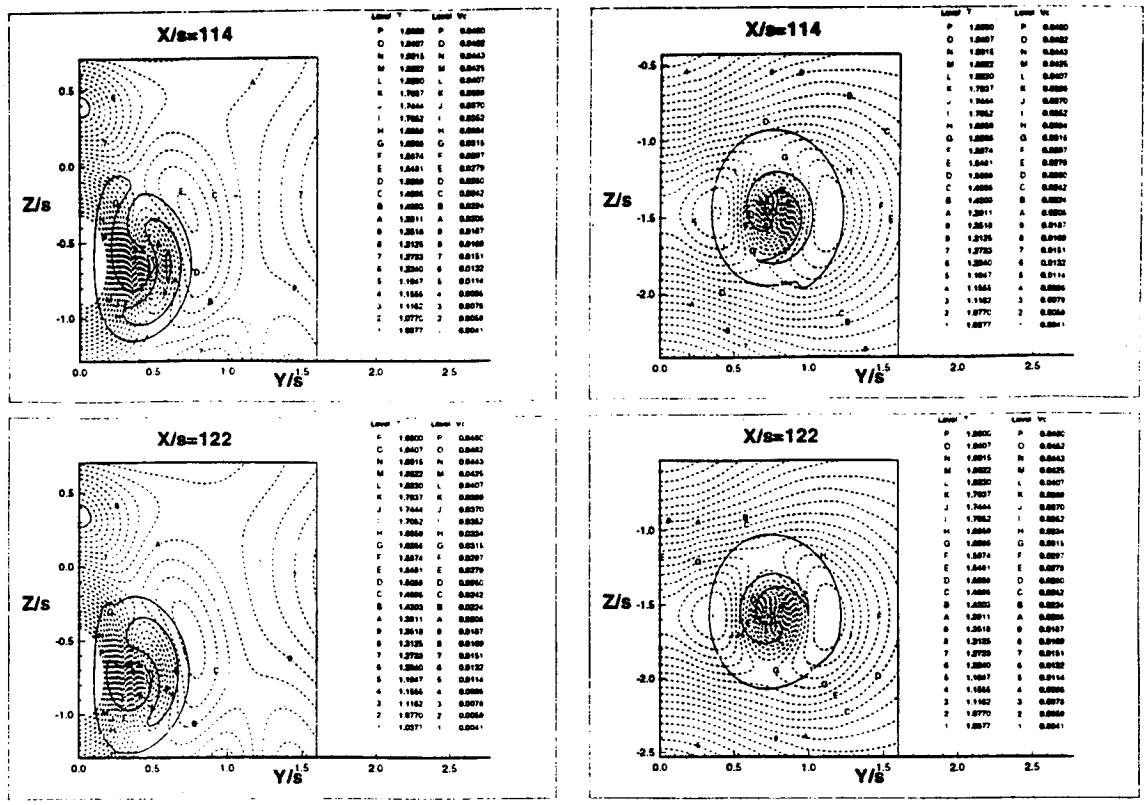

Figure 5: Comparison of crossflow T and Vc contours at two downstream stations; left-FTNS3D, and right-UNIWAKE. (One-side flowfield).

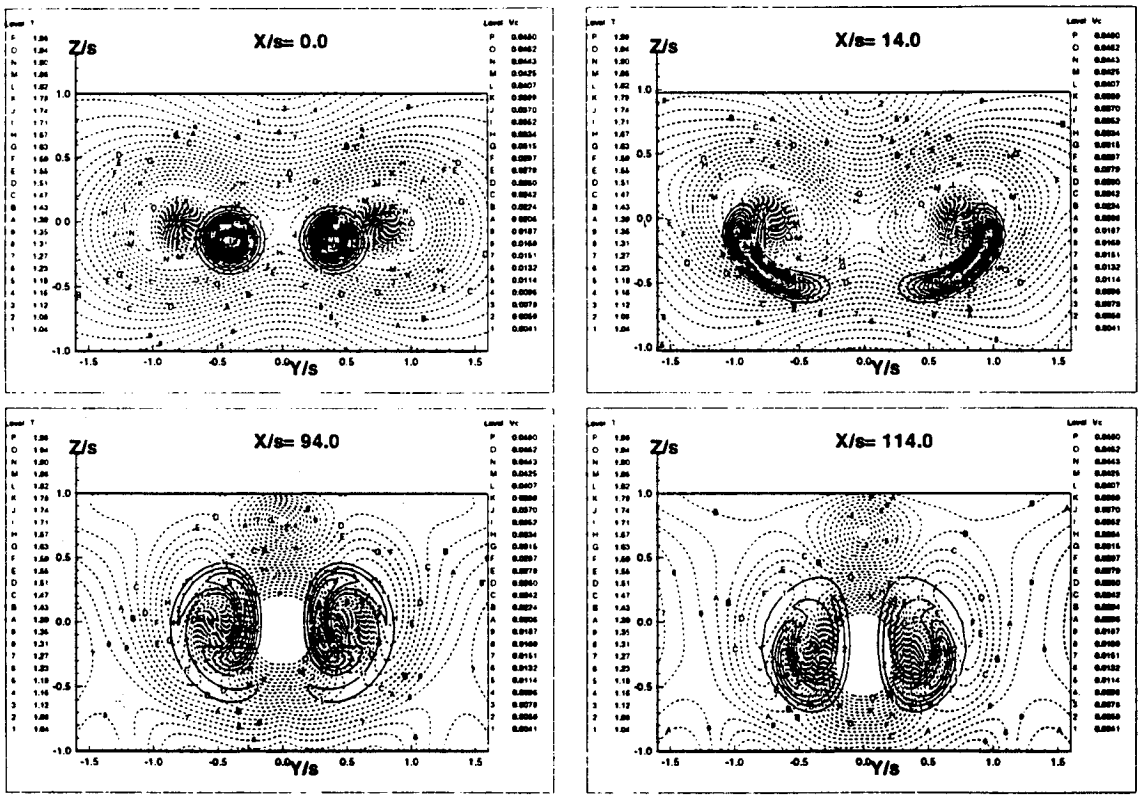

Figure 6: Crossflow T and Vc contours at four downstream stations. (Two-sides flowfield).

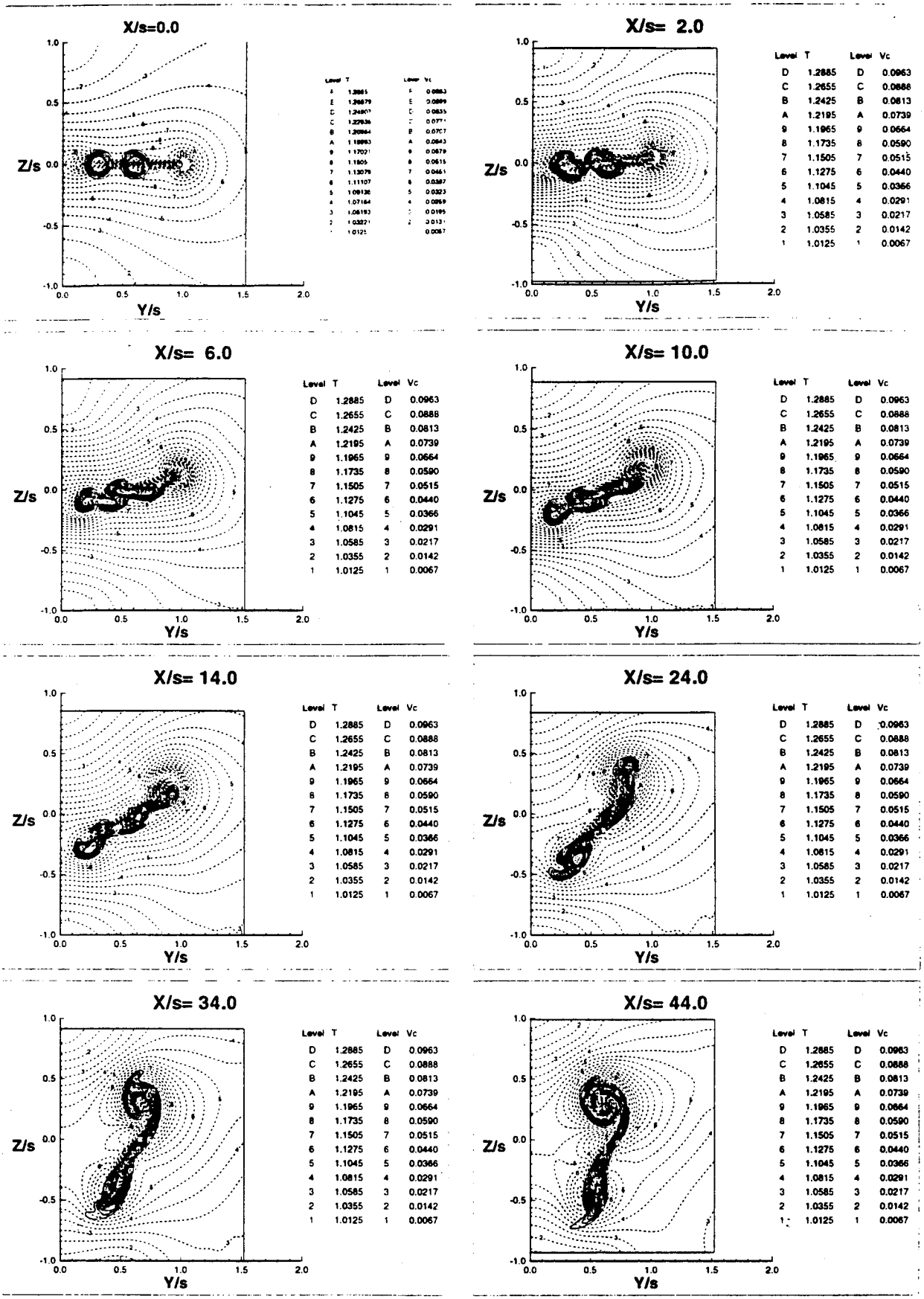

Figure 7: HSCT crossflow T and Vc contours at eight downstream stations. (One-side flowfield).

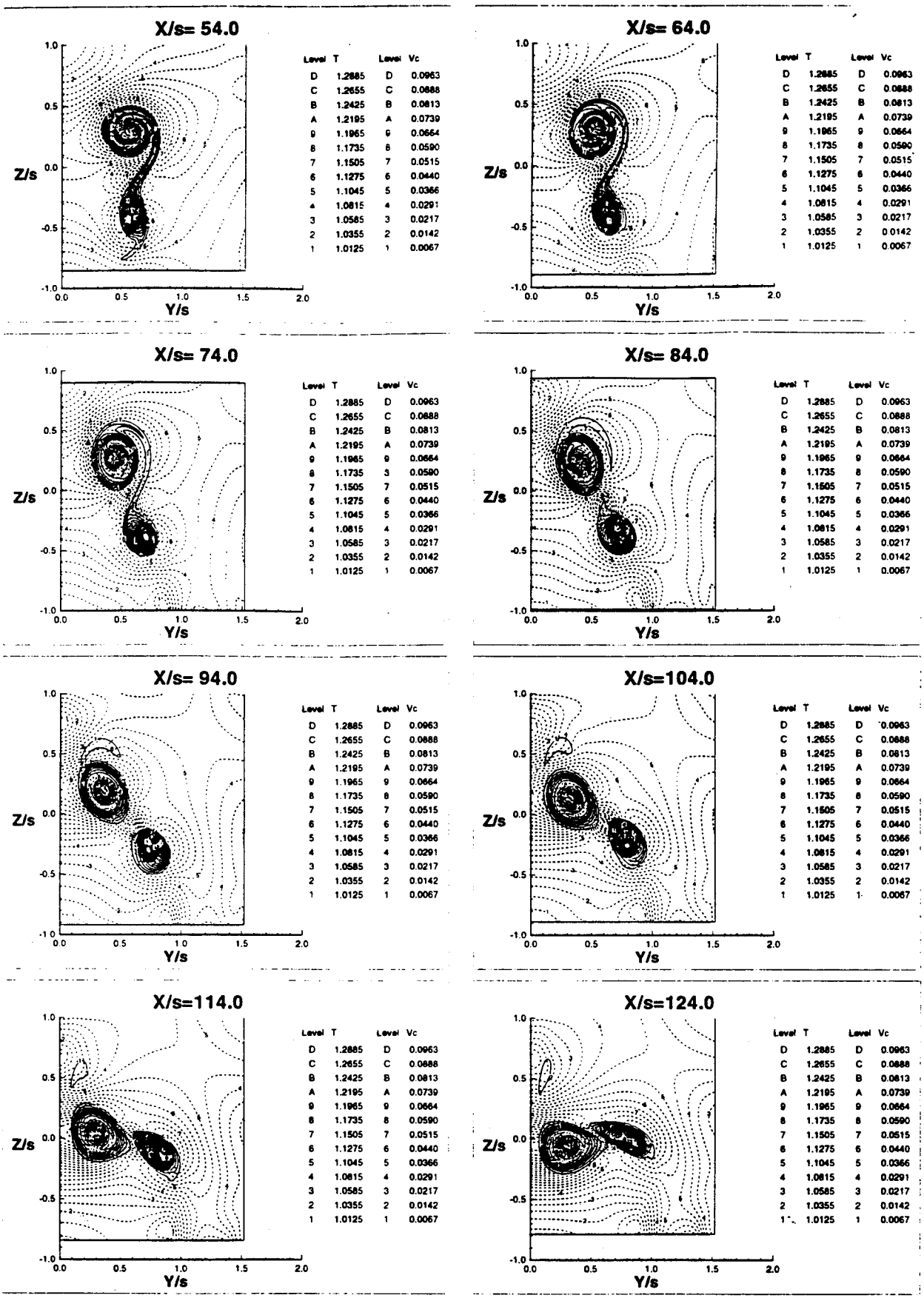

Figure 8: HSCT crossflow T and Vc contours at eight downstream stations. (One-side flowfield).

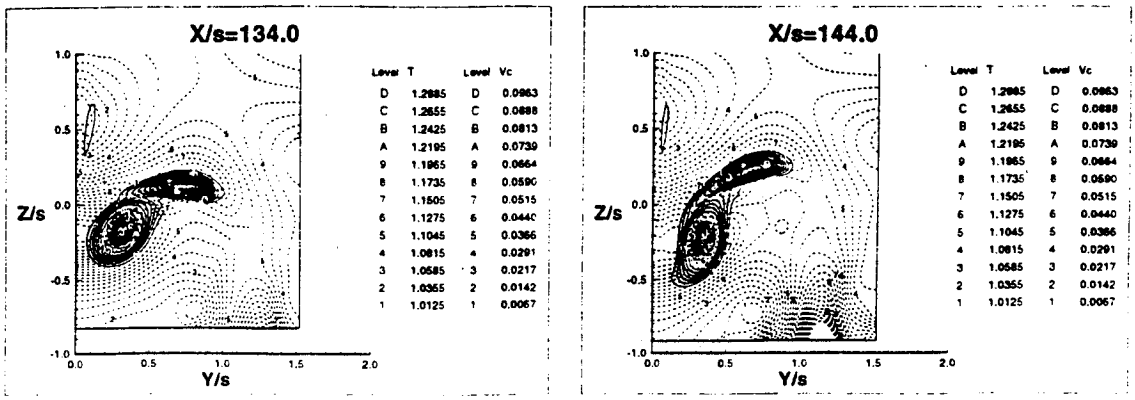

Figure 9: HSCT crossflow T and Vc contours at two downstream stations. (One-Side flowfield).

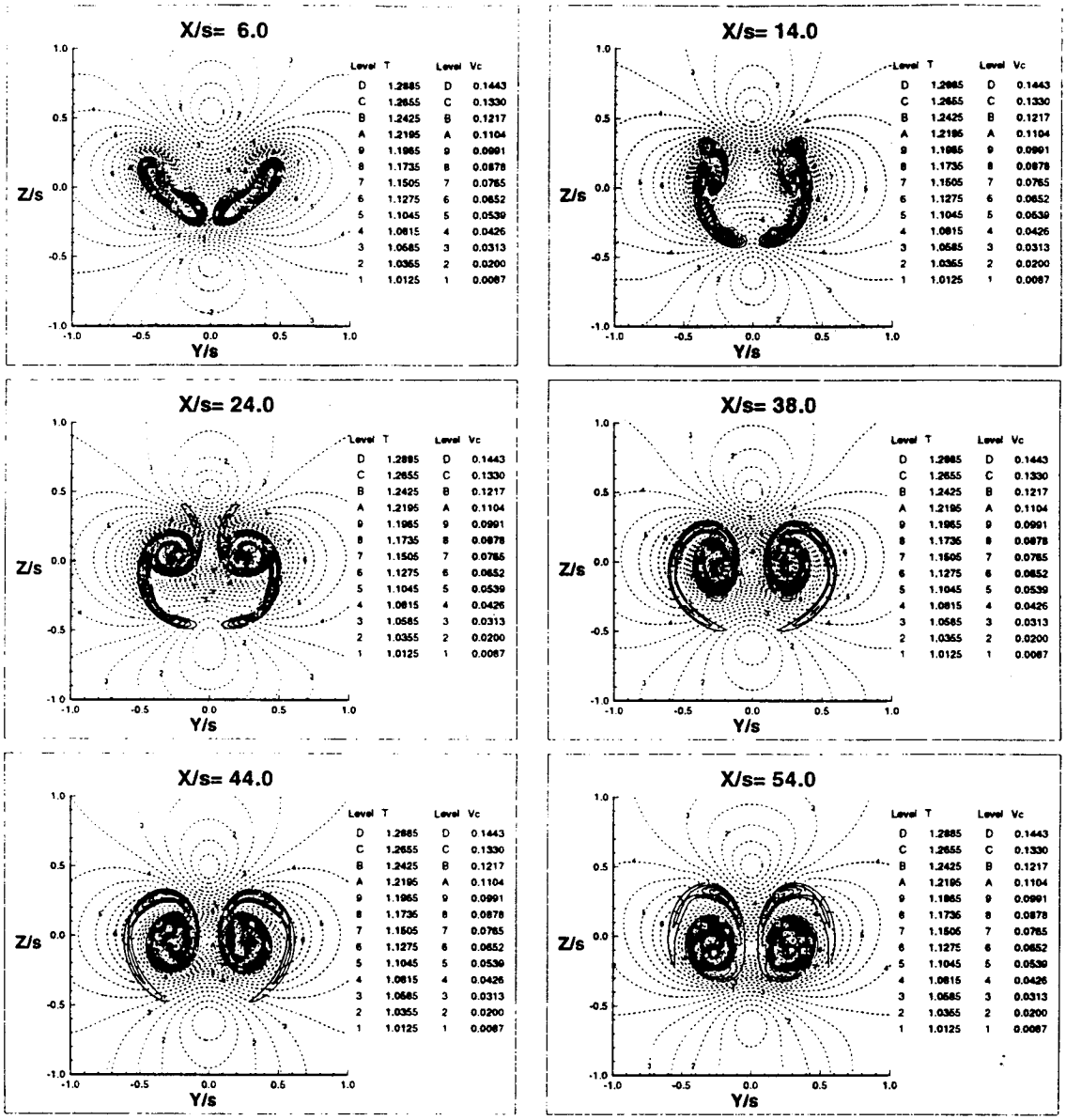

Figure 10: HSCT crossflow T and Vc contours at downstream stations. (Two-sides flowfield with reduced lateral separation distance).